ICARUS **133,** 221–232 (1998)
ARTICLE NO. IS985927

Near-Infrared Spectroscopy of Low-Albedo Surfaces of the Solar System: Search for the Spectral Signature of Dark Material

C. Dumas[1] and T. Owen

Institute for Astronomy, University of Hawaii, 2680 Woodlawn Drive, Honolulu, Hawaii 96822
E-mail: dumas@ifa.hawaii.edu

and

M. A. Barucci

Observatoire de Paris-Meudon, DESPA, 5, Place Jules Janssen, 92195 Meudon Cedex, France

Received June 30, 1997; revised February 9, 1998

We obtained I–J–H–K band spectroscopy of 18 low-albedo objects of the Solar System using the University of Hawaii 88-in. telescope equipped with the near-infrared spectrograph KSPEC. Most of our targets were selected from among the population of the Cybele, Hilda, and Trojan groups of asteroids, based on their low albedos and the relatively steep slopes of their reflection spectra at visible wavelengths. The outer jovian satellite Himalia and the Apollo object 3200 Phaethon were also observed. None of the spectra show absorptions similar to those found in the spectrum of 5145 Pholus, which remains the only asteroid-like object whose H–K band reflection spectrum contains a few broad absorptions due to organics. The near-infrared slope and the (1.0- to 2.2-μm) infrared color-index have been derived for each surface. This sample of primitive objects of the Solar System can be interpreted in terms of cometary-like objects that have undergone different degrees of aging.

Key Words: **infrared spectroscopy; asteroid and comet surfaces; composition; origin.**

1. BACKGROUND

Low-albedo asteroids (C, P, and D types) and comets contain a considerable amount of information regarding some of the primordial processes that governed the formation of the early Solar System planetesimals. But the connection between these two species is poorly understood. The physical distinction between asteroids and comets is simple: the surfaces or subsurface layers of comets retain volatiles that sublimate as the comets approach perihelion, while the external layers of asteroids do not. But if no cometary activity is detected, the observations alone cannot rule out a cometary nature. Indeed, some ''dormant-comet'' candidates behave like asteroids. These asteroid-like objects are considered dormant comets because their dynamical characteristics (high eccentricity and/or inclination) are similar to those of a cometary orbit (e.g., 944 Hidalgo) or because their trajectory is associated with some meteor streams (e.g., 2101 Adonis, 3200 Phaethon). Other objects, first considered to be asteroids, have also been revealed to be comets. This is the case for the Centaur 2060 Chiron (Hartmann *et al.* 1990, Meech and Belton 1990). The planetesimals 5145 Pholus is intriguing since its extremely red color (Mueller 1992, Tholen 1992) and low albedo ($p_v \sim 0.04$) (Davies *et al.* 1993a) may well be signs of a primitive, organic-rich surface (Cruikshank *et al.* 1997). The same compositional characteristics are expected from a distant comet nucleus that has never produced a coma in its lifetime. But Pholus, whose perihelion is located just beyond the orbit of Saturn, does not show any sign of activity, while Chiron does. The absence of a coma for Pholus cannot be explained simply by a heliocentric distance (r) that is large compared to Chiron's, since r_{Chiron} is currently 8.4 AU, while r_{Pholus} is 11.3 AU (Meech (1991) observed an outburst from comet P/Halley while r_{Halley} was 14.3 AU). We will come back to the differences between Chiron and Pholus later.

Main-belt asteroids have compositions that vary radially with heliocentric distance (Gradie and Veverka 1980) and the actual compositional trend of the asteroid population may indicate the different thermal histories undergone by solar nebula material (Gradie and Tedesco 1982). The

[1] Originally affiliated to the Observatoire de Paris-Meudon (DESPA) and junior visiting scientist at the University of Hawaii (IfA).

0019-1035/98 $25.00

inner part of the asteroid belt is dominated by fragments of differentiated asteroids (S and M types), followed by the metamorphosed asteroids (C type and subtypes), whose population density shows a peak at mid-distance through the belt. The outer region (semimajor axis, $a \geq 3.3$ AU) is mainly populated by groups of P- and D-type asteroids that have the lowest albedo ($p_v \leq 0.05$) and have probably not undergone much thermal and geological evolution. This compositional trend is also observed at a larger scale in the Solar System. In the saturnian system, the satellite Phoebe ($p_v = 0.06$) and the leading side of Iapetus ($p_v = 0.04$) are coated with dark material. Dark material covers the surfaces of the small inner satellites of Uranus. The rings of Uranus are also made of low-albedo material ($p_v = 0.03$) and are among the darkest objects in the Solar System. The estimation of the albedo of the Neptune ring/arc system from the Voyager images (Porco *et al.* 1995) is still somewhat uncertain, but some of the rings could be made from larger particles (diameter ≥ 500 μm) having an albedo p_v between ~ 0.032 (Le Verrier ring) and ~ 0.055 (Egalité arc of the Adams ring). Their composition seems close to that of ''dirty'' ice (Ferrari and Brahic 1994), although a silicate nature cannot be ruled out. Neptune's inner satellites are also coated with dark material (Thomas *et al.* 1995) with $p_v \in [0.056–0.063]$, similarly to P type asteroids in albedo.

Among the most primitive asteroids (C, P, and D types), the D-type asteroids display a steep slope in the visible and near infrared (V/NIR) while the C-type asteroids have neutral reflectance in this range. The P-type asteroids form a transition group between G- and D-type asteroids (Tholen and Barucci 1989, Barucci and Fulchignoni 1990). P- and D-type asteroids have been recognized as the most primitive (Barucci *et al.* 1987; Bell *et al.* 1989). Their red color cannot be explained by a rocky or icy surface. Vilas and Smith (1985) suggested that the increase in reddening of asteroid surfaces with heliocentric distance might be due to the increase in the number of hydrogen atoms in the molecules of compounds of their surface. P- and especially D-type asteroids are thought to have formed at low temperature in an organic-rich region of the solar nebula; Gradie and Veverka (1980) explained their low surface reflectivity by the presence of organic material. Some other authors (Cruikshank *et al.* 1991, Moroz *et al.* 1991, 1992) suggested that organics could be the cause of the low albedo and red color even if no conclusive spectroscopic evidence for organics has been observed. Jones *et al.* (1990) proposed a scenario for producing low-albedo asteroids: accretion of ice and anhydrous silicates from the solar nebula, combined with relic interstellar organic kerogen. The end-products are very dark, volatile-rich objects, of which the P- and D-type asteroids may be representative. These objects accreted at larger heliocentric (≥ 3.0 AU) than the metamorphosed C-type asteroids, and the water ice contained in the P and D asteroids could not melt and produce water of the hydration on their surfaces—although they may preserve ices and nearly unaltered solids and volatiles in their interiors.

D-type asteroids are found almost exclusively in the two Trojan swarms of asteroids that accompany Jupiter. Broadband visible photometry (Hartmann *et al.* 1987, Luu and Jewitt 1996) and visible spectroscopy (Jewitt and Luu 1990) showed that cometary nuclei have colors similar to those of the Trojan asteroids. Color studies of Centaurs and Kuiper belt objects (KBOs) by Luu and Jewitt (1996) and Davies *et al.* (1996) reveal that the color dispersions of KBOs and Centaurs are comparable. Visible spectroscopy of dark asteroids has also been carried out by Fitzsimmons *et al.* (1994) and by Lazzarin *et al.* (1995). They also compared the computed reflectivity gradients of dark asteroids with the known reflectivities of cometary nuclei and found no evidence of any distinction between the two populations. Despite the suspected presence of organics on their surfaces, the P- and D-type asteroids do not display any absorption features in their reflective V/NIR spectra and no clear features due to particular hydrocarbons or hydrated minerals have been found on D-type asteroids (Lebofsky *et al.* 1990, Britt *et al.* 1992). Several observational campaigns, performed by Luu *et al.* (1994), Barucci *et al.* (1994), and Lazzarin *et al.* (1995) to search for evidence of organic materials among dark asteroids, led to the same negative result. Cruikshank *et al.* (1991) reported infrared spectrophotometry data of several dark objects (asteroids, comets, Uranus rings) obtained by various observers. They attributed to C≡N-bearing organics a 2.2 μm feature visible in the spectra of the asteroids 1172 Aneas and 773 Irmintraud. Later, this absorption was not confirmed by Luu *et al.* (1994). Owen *et al.* (1995) failed to confirm the existence of this same feature on Iapetus reported by Cruikshank *et al.* (1991) and this work does not confirm the same absorption that Cruikshank *et al.* detected on the asteroid 368 Haidea. It appears that the observations in the Cruikshank *et al.* (1991) paper suffered from some systematic effect that produced spurious absorption at 2.2 μm.

Only the Centaur 5145 Pholus displays strong absorption bands in the near-infrared (Davies *et al.* 1993b). These features are commonly attributed to organic molecules but there are as yet no convincing identification. 5145 Pholus is one of the reddest objects known in the Solar System (Fink *et al.* 1992), with a 0.5- to 1.0-μm color index of ~ 1.4 magnitudes (the Centaur 1993 HA_2 and the KBO 1994 ES_2 have visible color indices similar to that of Pholus). A spectrum of 5145 Pholus of better quality than that which Davies *et al.* (1993b) obtained has been recorded by Luu *et al.* (1994), confirming the presence of broad absorption features at 2.07 and 2.27 μm and a weak feature at 1.72 μm. We shall adopt this spectrum as a reference and see whether any other dark, reddish asteroids exhibit

similar absorptions. A first attempt to identify these features has been made by Cruikshank *et al.* (1993). They attributed these spectral bands to the presence of aliphatic-rich and high H/C solid asphaltite-like organics on Pholus. Luu *et al.* (1994), after comparison with several laboratory spectra, found a partial match with absorption features of tar sand and N−H bonds. Wilson *et al.* (1994) found a fairly good match for the Pholus absorption bands using a mixture of HCN polymer, tholin, and ammonia ice. Owen *et al.* (1995) mention that none of these organic mixtures return good fits for all three absorption features detected in the reflection spectrum of Pholus, although the weak 1.7-μm feature detected by Luu *et al.* (1994) needs to be confirmed. The best match for the Pholus absorption bands was recently obtained by Cruikshank *et al.* (1997) with a mixture of water ice, methanol, and/or its photo-dissociation product.

The transneptunian objects that populate the outer regions of the Solar System may have built irradiation mantles (Luu and Jewitt, 1996). The surfaces of these bodies have been exposed to solar ultraviolet radiation and cosmic ray bombardment for 4.6 billion years, which could have dissociated the icy molecules down to several meters of the planetesimal regolith (Thompson *et al.* 1987), possibly creating some new organic molecules in the process. One can argue that the Trojan asteroid should also have such irradiation mantles. In this case, however, the lack of any detectable spectral feature might be due to such a high level of alteration by solar radiation that the organics present on their surfaces no longer show discrete spectral features.

Is there a unique explanation for the diversity of colors displayed by the most primitive objects of the Solar System: dark asteroids, cometary nuclei, Centaurs, and KBOs? What is the nature of this dark material? Is it always the same or are there different varieties? Our comprehension of dark matter in the Solar System is directly linked to the spectrophotometric data available for the most primitive objects. Recent progress in the sensitivity of detectors makes near-infrared spectroscopy of objects with low albedo acessible from the ground. Studies that investigate the nature of the dark matter in the Solar System (e.g., Cruikshank 1987, Owen *et al.* 1995) need to be pursued in order to understand better the boundary between comets and primitive asteroids. This paper presents the results of a survey obtained on a sample of 18 primitive objects. Near-infrared spectroscopy (0.9–2.5 μm) of these objects was carried out on the University of Hawaii 2.2-m telescope in order to search for the spectral signatures of organics on their surfaces.

2. OBSERVATIONS

2.1. Instrumentation

The observations were performed using the K-band spectrograph KSPEC (Hodapp *et al.* 1996) built at the Institute for Astronomy of the University of Hawaii. This version of KSPEC uses a 1024 × 1024 HgCdTe array for spectroscopy in the 0.8- to 2.5-μm range and a 256 × 256 NICMOS array for K-band imagery of the region surrounding the slit. KSPEC is a cross-dispersed spectrograph optimized for the K band, each order having a different degree of curvature. The level of dark current is relatively low ($\sim$0.1 e/s^{-1}). Several widths were available for the slit. We used the 0.″96-slit primarily for our runs except during September 95, when we used a slit of 0.″56. The resolution varies from 250 to 1500 for the K band, depending on the slit width adopted. The resolution at 2.2 μm for the 0.″96 slit is $\sim$700.

All data except the observations of Phaeton were recorded using a tip-tilt mirror in order to compensate in real time for telescope vibrations and the first order of the atmospheric turbulence. A dichroic lens directs the light to a wavefront sensor. This tip-tilt correction can be done by locking the wavefront sensor onto a nearby star (within a few degrees of the science object) whose V_{mag} can be as faint as 14th or by using the object itself, which ensures the best correction while preventing wavelengths shorter than 0.9 μm from reaching the spectrograph.

2.2. Observing Procedures

Dome flat-fields were recorded at the beginning and end of each night using incandescent and fluorescent lights. In order to spend the maximum amount of time integrating on the science object, sky frames were not systematically recorded. Instead, the sky level was fitted by extrapolating the background level from each side of the object. To diminish the alteration of our data set by the bad pixels present on the chip, the spectrum of the object was recorded at different locations on the array. This was achieved by dithering the object along the slit between each exposure. Some selected G-dwarfs (list of rough solar analogs provided by T. Geballe) from the Yale Bright Star Catalog were frequently visited to derive the relative spectral reflectivity of our objects. Wavelength calibration was done using an argon lamp except in the case of 3200 Phaethon, for which OH^- sky emission lines (Ramsay *et al.*, 1992) were used.

2.3. Reduction

An IDL software package, optimized for the extraction of low S/N spectra, was developed to reduce this data set. This solution was prefered for its flexibility and also because the pre-existing IRAF reduction package does not provide any correction for the high frequency noise present in the KSPEC data.

The first task is to correct each frame for bias defects and bad pixels. Two bad pixel masks are defined. A bad pixel mask for the faint objects (science objects) is realized

by taking into account most of the bad pixels on the chip. Another bad pixel mask is defined using the location of the brightest bad pixels only. This second mask is intended to correct the frames containing the spectrum of the bright solar analog stars.

Several dark and bright flat fields were recorded at the end of each night of observation. A unique dark flat field is obtained by taking the median of all the dark dome-flats and the same procedure is done for the bright dome-flats. The final flat is then realized by normalizing the difference of the bright and dark flat fields.

We then define the curvature and border of the different orders on the chip and subtract the sky for each order by fitting its level. This technique yields a very clean image compared to the subtraction of a sky frame that suffers from the temporal variation of the brightness of the OH sky lines. The power spectrum of the object is low-pass filtered in Fourier space in order to remove the pixel-to-pixel noise introduced by our sky subtraction technique. For each order, we combine all the spectra to obtain a mean spectrum and a median spectrum. Due to the higher S/N of the mean spectrum, we replace only those portions of the mean spectrum affected with bad pixels with the corresponding portion of the median spectrum. The latter is first scaled to the mean spectrum. Each object spectrum is then divided by the spectrum of a solar analog in order to get the relative spectral reflectance of the object surface. We noticed that despite the flatfield and the division by a solar analog, pattern noise introduced by the readout of the four quadrants of the spectrograph array was still present in the final spectrum. Fourier analysis of this noise showed that its frequency varied over the surface of the array and was not constant in time. We designed a bandpass filter for each order that attenuated only a certain range of spatial frequencies. Typically this noise had a periodicity of 5–10 pixels along the K band order. Also, due to the poor quality of the chip close to the bottom edge, the signal of the faintest source was highly altered by the bad pixels present at this location. Therefore, the signal around 2.0 μm, where the water band absorption is the strongest, is quite noisy. For the data obtained during the September 1995 observing run, the K band order was located higher on the chip, and this data-set is less affected by bad pixel noise than the 1996 observations.

3. RESULTS

3.1. Selection of the Candidates

Table I contains the physical and observational characteristics of the objects selected for this study as well as the dates and integration times used for the observations. We selected our targets on the basis of their low IRAS albedo (Tedesco *et al.* 1992) and/or their taxonomic class (P or D types). Another criterion was to select the objects based on the high color-index in the 0.55- to 1.04-μm range ($v-z$ color index) obtained from the ECAS catalog (Zellner *et al.* 1985) in order to approach the very steep slope of Pholus' reflection spectrum in the visible. Most of the objects we observed (table I) are orbiting beyond the external edge of the main belt defined by the 2 : 1 orbital resonance with Jupiter and belong to the Cybele, Hilda, or Trojan groups. Exceptions in our list are 72 Feronia, whose orbit is located at the inner edge of the main belt (a = 2.3 AU) and which is one of the darkest asteroids of the belt; 368 Haidea and 838 Seraphina, with semimajor axes of 3.1 AU and 2.9 AU, respectively; and 3200 Phaethon, which belongs to the Apollo family of Earth-crossing asteroids. We also observed Himalia (J_{VI}), the brightest of the outer irregular Jovian satellites. All the asteroids are low-albedo objects, whose class is either P or D except for Phaethon, which is classified F in the Tholen taxonomy, and Jupiter's satellite Himalia, whose surface is considered similar to that of a C-type asteroid by Tholen and Zellner (1984) and Luu (1991).

3.2. Discussion

3.2.1. Description of the Spectroscopic Data Set

The reflectance spectra of the 18 objects observed with KSPEC are shown in Fig. 1 with the H–K band spectrum of 5145 Pholus (Luu *et al.* 1994) overplotted for comparison. The H–K band reflection spectrum of 2060 Chiron (Luu *et al.* 1994) is also reproduced in Fig. 1.19. Each spectrum has been normalized at 2.2 μm. The wavelength coverage of KSPEC varies depending on the setup of the instrument which was different for the September 1995 data and the March and September 1996 data. The spectrum of 3200 Phaethon (Fig. 1.17) was recorded on December 1994 using the previous version of KSPEC (Hoddapp *et al.* 1994) which only had a 256 $\times$ 256 Nicmos array. Its resolution is lower than that for the rest of the data set.

The J_2 order (1.2–1.35 μm) is noisy and useless for any target fainter than ~14.5 magnitude. This part of the spectrum is not shown for 1512 Oulu (Fig. 1.3) and 3451 Mentor (Fig. 1.9). In addition to this, the 2.0-μm region of the spectra is altered by a cluster of bad pixels present on the chip at this location and also because the signal is weak around 2.0-μm due to the atmospheric water vapor absorption bands. Fortunately for this study, Table II shows that the best S/N at the K band is obtained between 2.2 μm and 2.3 μm, where the strongest absorption bands of Pholus are located. The estimated S/N is in the range 30–125.

Figure 1 shows that the reflectance spectra obtained are either nearly flat or redder than the solar analog spectrum and do not contain any spectral feature similar to Pholus. The spectra of 838 Seraphina (Fig. 1.2) and 1512 Oulu (Fig. 1.3) contain a shallow and broad absorption in H

TABLE I
Physical and Observational Characteristics of the 18 Primitive Solar System Objects Observed

Object name	Semi-major axis (AU)	IRAS[a] albedo (p_v)	v–z color-index[b] [0.55 - 1.04]μm	Group	Type	Observation dates	Magnitude (V)	Exposure (sec.)
72 Feronia	2.3	0.063	—	—	TDG	06 Sep 95	11.2	1500
153 Hilda	4.0	0.062	0.13	Hilda	P	09 Mar 96	14.6	2400
368 Haidea	3.1	0.039	0.32	—	D	02 Sep 96	13.5	3600
420 Bertholda	3.4	0.042	0.24	Cybele	P	02 Sep 96	14.4	6000
588 Achilles	5.2	0.033	0.36	Trojan	DU	02 Sep 96	15.6	6000
624 Hektor	5.2	—	0.42	Trojan	D	13 Sep 95	14.4	3000
748 Simeisa	3.9	0.042	0.11	Hilda	P	11 Sep 95	15.1	4800
838 Seraphina	2.9	0.046	0.20		P	06 Sep 95	14.1	2400
911 Agamemnon	5.2	0.044	—	Trojan	D	02 Sep 96	15.0	8400
1180 Rita	4.0	—	0.15	Hilda	P	31 Aug 96	14.6	5100
1212 Francette	4.0	0.040	0.16	Hilda	P	09 Mar 96	14.2	5700
1512 Oulu	3.9	0.037	0.17	Hilda	P	07 Sep 95	15.4	4800
1578 Kirkwood	3.9	0.051	0.45	Hilda	D	03 Sep 96	15.6	10800
1746 Brouwer	3.9	0.045	0.42	Hilda	D	13 Sep 95	15.1	7200
2312 Duboshin	3.9	0.050	0.44	Hilda	D	13 Sep 95	15.6	6000
3451 Mentor	5.1	—	—	Trojan	—	09 Mar 96	15.5	8100
Himalia (JVI)	5.2	0.03[c]	—	—	—	03 Sep 96	~15.5	9600
3200 Phaethon	—	0.098	—	Apollo	F	18 Dec 94	14.7	2280

[a] Tedesco *et al.* (1992).
[b] Zellner *et al.* (1985).
[c] Cruikshank (1977).

band and 2312 Duboshin (Fig. 1.6) displays another shallow absorption near 2.2 μm. These features require confirmation and could be due to an incomplete compensation of the atmospheric absorption (Seraphina and Oulu) or removal of the bad pixels (Duboshin). All other features visible in the spectra of our selected objects can be explained by the noise resulting from an incomplete correction of the bad pixels, especially near 2.0 μm.

TABLE II
Signal-to-Noise Ratio Achieved and Near-Infrared Color-Index Measurements

Object name	Estimated S/N at 2.2μm	[1.0μm - 2.2μm] color-index
72 Feronia	75	0.14 ± 0.03
153 Hilda	49	0.28 ± 0.03
368 Haidea	97	0.45 ± 0.04
420 Bertholda	58	0.62 ± 0.04
588 Achilles	32	0.60 ± 0.03
624 Hektor	58	0.54 ± 0.03
748 Simeisa	34	0.20 ± 0.07
838 Seraphina	75	0.42 ± 0.02
911 Agamemnon	43	0.64 ± 0.04
1180 Rita	42	0.21 ± 0.04
1212 Francette	125	0.34 ± 0.03
1512 Oulu	61	0.19 ± 0.04
1578 Kirkwood	32	0.34 ± 0.03
1746 Brouwer	64	0.11 ± 0.03
2312 Duboshin	45	0.65 ± 0.04
3451 Mentor	49	0.31 ± 0.04
Himalia (JVI)	30	0.02 ± 0.03
3200 Phaethon	45	—

3.2.2. Near-Infrared Slope and Color-Index

Each reflectance spectrum was smoothed with a boxcar average of 21 pixels (resolution ~200) to remove the high frequencies of the signal. Each smoothed spectrum was then least-squares fitted with a polynomial to derive the general slope of the spectrum. In Fig. 2 we plot the slope of the reflection spectrum obtained for each object in order of increasing redness. Himalia, the most neutral surface, is plotted at the bottom. The reddest objects, 2312 Duboshin, 911 Agamemnon, 420 Bertholda, and 588 Achilles, are distributed among the three outer groups, Cybele, Hilda, and Trojan, and are classified as D- and P-type asteroids in the Tholen classification. A 1.0- to 2.2-μm color-index was derived from the slope of each spectrum. Table II reports these infrared color-indices and Fig. 3 is a plot showing the 1.0- to 2.2-μm color-index of each object versus its respective semimajor axis. The derived infrared color-indices vary from 0.02 to 0.65 magnitudes (Himalia and Duboshin respectively). 2312 Duboshin, the only object whose reflection spectrum shows a possible shallow absorption at the K band, has the highest visible and infrared color-indices among the 18 observed objects. Our sample contains mainly P- and D-type objects with the exception of 3200 Phaethon and J_{VI} Himalia. Although this

sample is too small to be representative of the distribution of low albedo asteroids in the outer belt, Fig. 3 shows that the mean infrared color-index of the observed Trojans is higher than the mean color-index of the objects we have selected from the Hilda group.

3.2.3. The Case of 368 Haidea and 3200 Phaethon

The spectrum of 368 Haidea in Fig. 1.14 is particularly interesting since this asteroid was one of the three minor planets (the other ones being 1172 Aneas and 773 Irmintraud), for which Cruikshank *et al.* (1991) claimed detection of an absorption band near 2.2 μm that they attributed to the presence of C≡N-bearing solid material. Luu *et al.* (1994) previously reported that this absorption was missing in their spectra of 1172 Aneas and 773 Irmintraud. The reflection spectrum of 368 Haidea shown in Fig. 1.14 is featureless. The derived 1.0- 2.2-μm color-index is 0.45 magnitude for Haidea, a typical value for a D-type candidate.

Asteroid 3200 Phaethon is a particular case since it belongs to the Apollo group of Earth-crossing asteroids and is the parent body responsible for the Geminid meteor shower (Whipple 1983, Williams and Wu 1993). The "dead-comet" nature of 3200 Phaethon was strongly supported by the work of Hunt *et al.* (1985) who showed that only a comet nucleus could produce the observed distribution of aphelia for the Geminid shower. Also, the physical characteristics of the Geminid fireballs (Halliday 1988) are in agreement with those of a nonactive comet. Its surface is probably made of a rubble mantle (Whipple 1950), the end result of a near-total loss of volatiles. This model predicts that only the larger dust particles that cannot leave the nucleus remain on the surface of such a body. Initial spectrophotometry of 3200 Phaethon concluded that its surface is more like that of an S-type asteroid (Cochran and Baker 1984, Belton *et al.* 1985). These results were not confirmed by Veeder *et al.* (1984), who concluded that this object was extremely blue. Phaethon was observed on December 18, 1994, with the first generation of KSPEC (Hoddap *et al.* 1994). Its surface reflectance (Fig. 1.17) is slightly blue in H while neutral in K band. No spectral features are visible in this wavelength range. The spectrum resembles the dust continuum recorded from several comets like 2060 Chiron (Luu *et al.* 1994) (Fig. 1) or P/Schwassmann-Wachmann 1 (Owen *et al.* 1995). Figure 1 shows that the reflection spectra of 72 Feronia (Fig. 1.1) and 1746 Brouwer (Fig. 1.5) have slopes similar to that of 3200 Phaethon (Fig. 1.17) in the 1.0- to 2.5-μm region. The main difference between the spectra of these two main belt asteroids and 3200 Phaethon occurs in the visible range where the Apollo asteroid displays a blue reflectance while the spectra of Feronia and Brouwer are red.

3.2.4. A More Global Picture

We can find some clues as to why Trojan asteroids do not show any sign of organics on their surfaces by looking at outer Solar System objects such as Centaurs and KBOs.

Chiron and Pholus. 2060 Chiron and 5145 Pholus are probably KBOs (Duncan *et al.* 1988) perturbed into unstable, short-lived ($\sim 10^6$ years) orbits (Hahn and Bailey 1990) that cross the trajectories of the gas giant planets. Although it is reasonable to think that they originally came from the same reservoir, they do show totally different spectral characteristics in the V/NIR range (see the spectra of Pholus and Chiron in Fig. 1.19). The lack of activity of 5145 Pholus compared to 2060 Chiron can hardly be explained by the actual greater heliocentric distance of Pholus, since the current ratio of the solar flux density for both objects is only on the order of $(r_{\text{Chiron}}/r_{\text{Pholus}})^2 \sim 0.5$. Although we do not know with certainty the nature of the sublimated volatile that is at the origin of Chiron's coma, it is reasonable to think that CO is the molecule responsible for its activity. Indeed, Delsemme and Miller (1971) showed that at larger heliocentric distances than 5 AU, CO ice can sublimate while H_2O cannot. Notesco and Bar-Nun (1996) have shown that CO trapped in amorphous ice, could power cometary activity at large distance from the sun more efficiently than N_2. If Pholus does expose icy molecules of CO (or N_2) to solar radiation, a coma should be detectable at this heliocentric distance.

Broadband visible color measurements on a sample of 9 KBOs by Luu and Jewitt (1996) showed that the slopes of their reflectance spectra cover a large range of values, the reddest (1994 ES_2) being as red as Pholus while the flattest (1995 QY_9) is almost as neutral as Chiron. They suggest that the large color dispersion among KBOs (and Centaurs) reflects the diversity of surface composition resulting from collisional resurfacing. KBOs formed in a region of the solar nebula where clathrate and pure methane could condense and Thompson *et al.* (1987) showed that UV irradiation of hydrocarbon-containing ices (such as CH_4 or CO clathrate) can transform these molecules into a red organic-rich mixture. If the irradiation level

FIG. 1. Near-infrared reflective spectra of the 18 primitive surfaces observed with KSPEC. The H–K band spectrum of Pholus (Luu *et al.* 1994) is overplotted for comparison. None of these spectra display absorption features that can be attributed to organics as in the case of Pholus. Any "features" present in these spectra can be explained by low S/N (J_2 order and 2.0- to 2.05-μm region). In addition to the objects observed in this study, we also plot in Fig. 1.19 the spectrum of Chiron from Luu *et al.* (1994).

72 Feronia

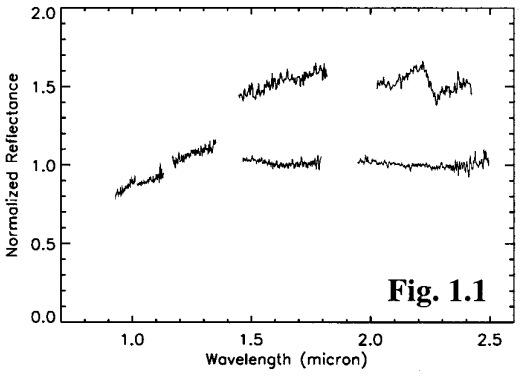

Fig. 1.1

838 Seraphina

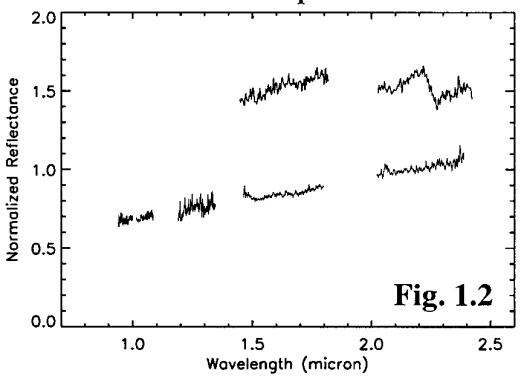

Fig. 1.2

1512 Oulu

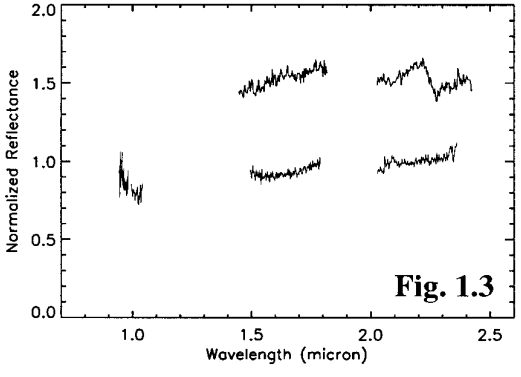

Fig. 1.3

748 Simeisa

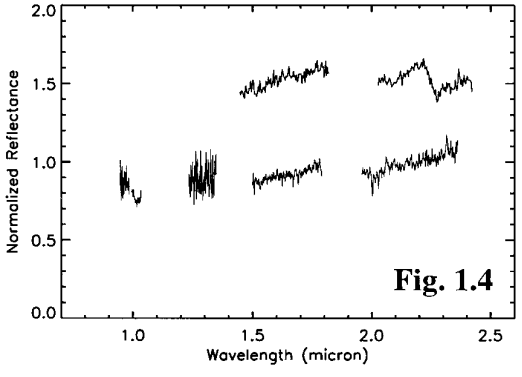

Fig. 1.4

1746 Brouwer

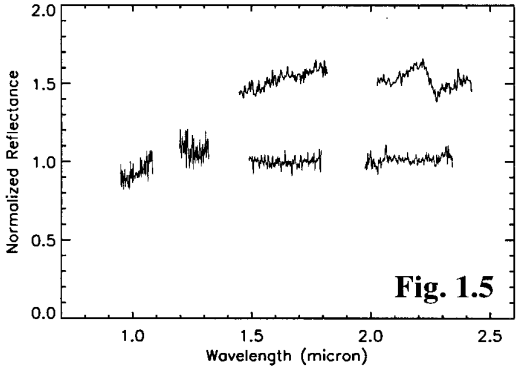

Fig. 1.5

2312 Duboshin

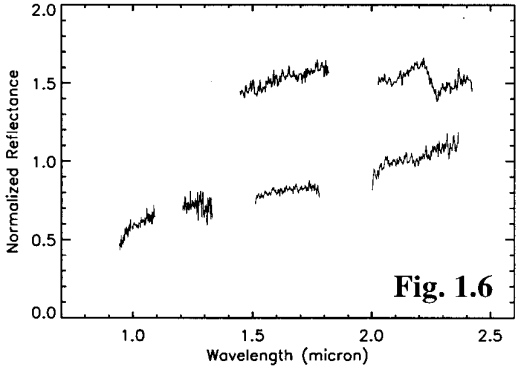

Fig. 1.6

624 Hektor

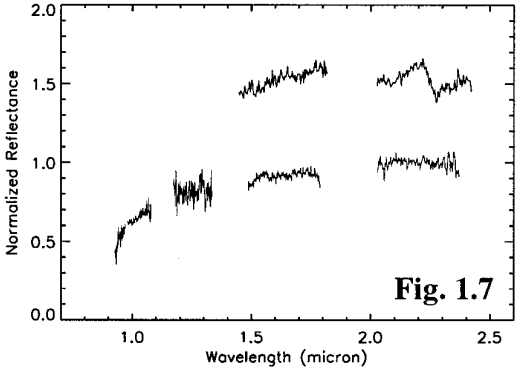

Fig. 1.7

1212 Francette

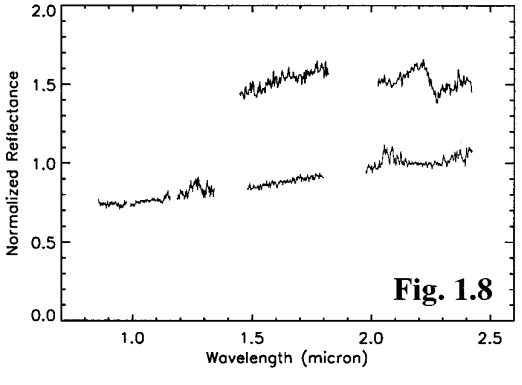

Fig. 1.8

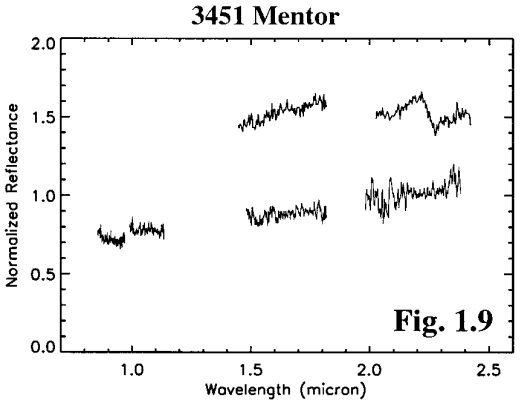

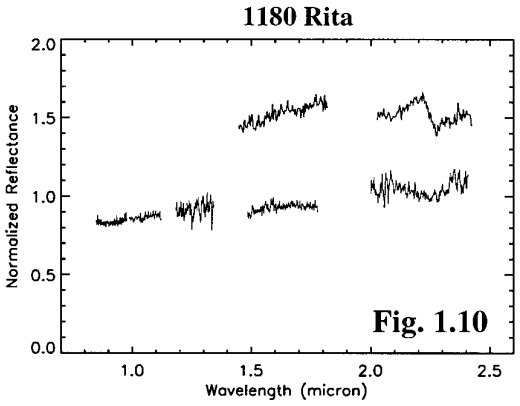

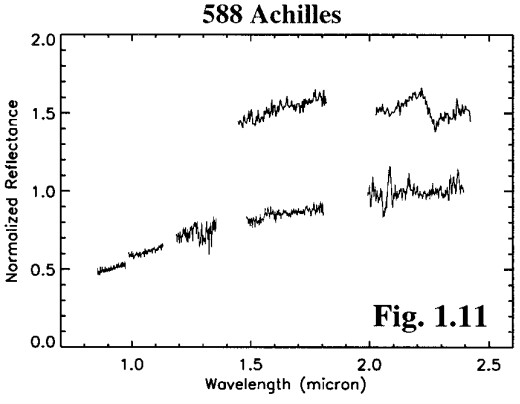

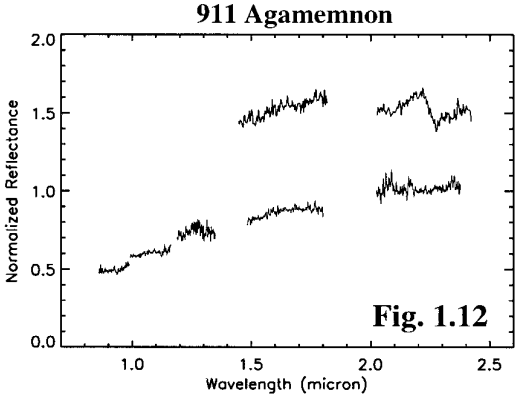

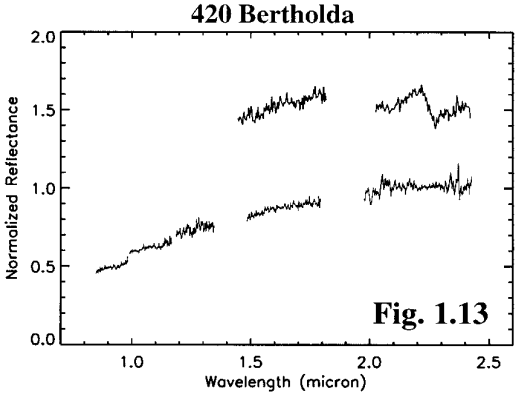

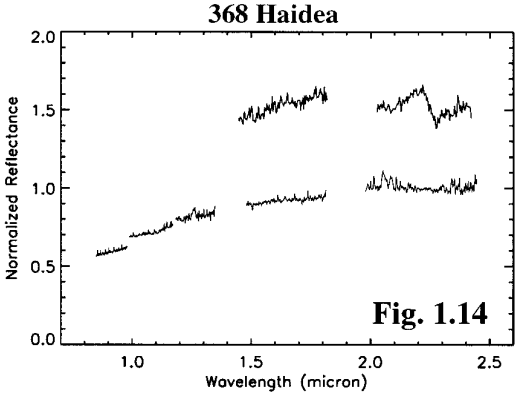

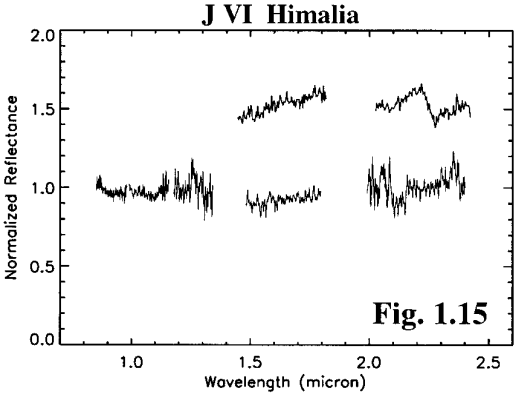

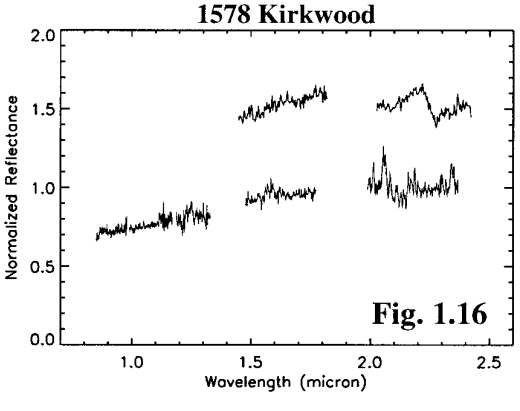

FIG. 1—*Continued*

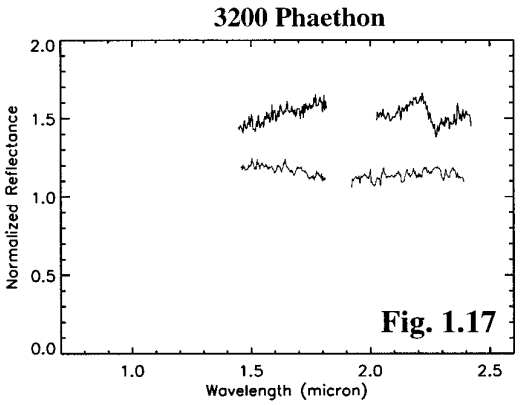

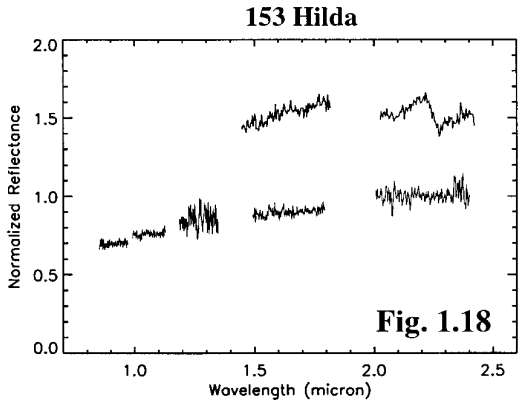

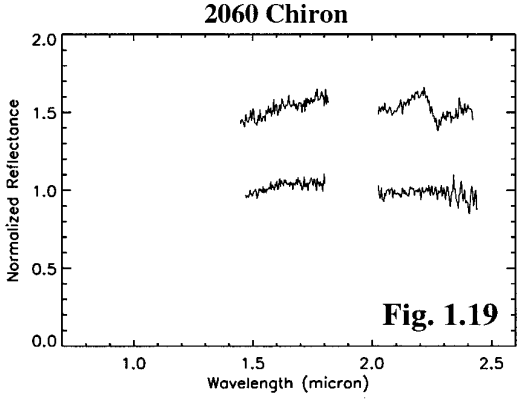

FIG. 1—*Continued*

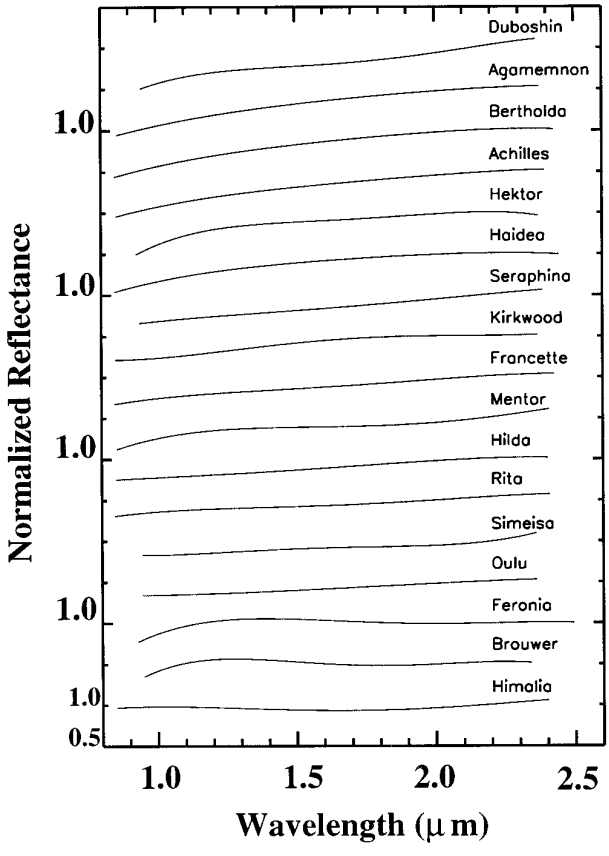

FIG. 2. Polynomial fit of the individual reflectance spectra plotted in order of increasing color-index from top to bottom (see Table II for color-index values). The plots have been shifted vertically by 0.5 unit for clarity. Himalia displays the most neutral surface while the objects having the steepest reflectance are distributed among the three outer groups of asteroids visited.

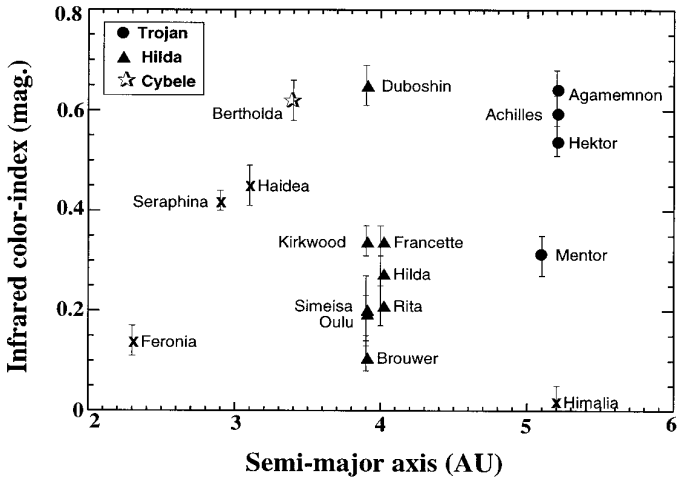

FIG. 3. The 1.0- to 2.2-μm color-index versus the semimajor axis for all the objects observed but Phaethon, for which we do not have I–J band spectra. In the figure, the symbol assigned to the Trojans is a full circle, the Hildas are represented by a triangle, and the unique Cybele observed (Bertholda) is denoted with a star. This plot do not show any particular concentration of spectrally red objects with regard to the heliocentric distance, although the mean infrared color-index of the observed Trojans is higher than the mean infrared color-index of the objects we have selected from the Hilda groups. The population of the Hilda and Trojan groups is heterogeneous and contains D-class as well as P-class objects. Note that Himalia has the lowest color-index of 0.02 magnitude, which confirms that this outer Jovian satellite has a surface similar to that of a C-type asteroid.

increases, the hydrocarbons lose their hydrogen atoms and the residual is a grey, spectrally almost flat carbon rich substance. Collisions in the Kuiper belt can partially bury an irradiation mantle, similar to the one on Pholus, in order to expose locally the inner mantle icy material, unprocessed by solar radiation and less red. This could explain why Pholus is not active and still shows the presence of organics on its surface (Cruikshank *et al.* 1997) while Chiron's surface is neutral and exhibits activity (Hartmann *et al.* 1990, Meech and Belton, 1990). Cruikshank *et al.* (1997) attribute the 2.04-μm absorption band in the spectrum of Pholus to the presence of H_2O ice molecules on its surface, which agrees with the work of Thompson *et al.* (1987), who showed that it is expected to find H_2O ice to be still present after irradiation of the mantle. To summarize, this picture suggests that 5145 Pholus and 2060 Chiron might in fact be very similar objects for which only the external layer differs. Another possible explanation for the differences between the two Centaurs, Pholus and Chiron, although more unlikely, is that Pholus has been perturbed into its chaotic orbit more recently than Chiron and its surface has not changed yet through the effect of increased solar UV irradiation.

Trojan asteroids. Similarly, Trojan asteroids might retain icy molecules in their interiors while their surfaces have been highly altered by solar UV and irradiation by cosmic rays and solar wind. The origin of the Trojan asteroids is still uncertain. They might have accreted in the solar nebula at their present locations or formed at larger heliocentric distances, becoming gravitationally trapped at the L_4 and L_5 Lagrangian points of Jupiter. In any case they were almost certainly formed in a region of the solar nebula rich in frozen volatiles. The relatively high level of irradiation undergone by the subsurface layers of these objects for the last 4.5 billion years might explain why near-infrared spectroscopy of their surfaces does not reveal any absorption features similar to those in the spectrum of Pholus. But it also raises another question. Why are most Trojans still red, after their surfaces have been exposed to irradiation for billions of years, while some supposedly more pristine outer Solar System objects, such as KBOs, display neutral reflectance? This question is even more forceful in the case of Duboshin and Bertholda (Fig. 3), whose semimajor axes are considerably smaller than those of the Trojans. Figure 2 shows that none of the Trojans observed has a neutral slope in the V/NIR region. Is there a mechanism that continuously supplies the surface with hydrocarbon/icy material on a time scale smaller than the time needed to turn this substance into pure carbon? If so, why do not we detect any spectral features due to organics? As is the case for the Kuiper belt, collisional resurfacing might happen in the Trojan swarms, replenishing the surfaces of these asteroids with icy molecules. Irradiation of this mixture of ice and carbon might explain why the reflection spectra of the Trojans still display a red slope in the visible and near-infrared. Jewitt and Luu (1990) and Fitzsimmons *et al.* (1994) showed that the smaller the diameter of a D-type asteroid, the redder is its visible reflection spectrum. An observational test for the presence of ice in the interior of the Trojans would be to obtain spectrophotometric data of the surface composition of the km-sized Trojans, which are produced by fragmentation of larger bodies and might therefore expose the mantle material. Also, the study presented here concerns only a small region of wavelengths. The spectral signatures of the dark material that covers the surfaces of primitive asteroids might be detectable at longer wavelengths, where the bands of ice and organics are stronger.

Near-infrared spectroscopy will soon be possible on 8- to 10-m telescopes which will allow us to better investigate the aging processes that are likely responsible for the state of the surfaces of primitive Solar System objects.

4. CONCLUSION

Near-infrared spectroscopy is potentially a powerful tool that can be used to characterize primitive surfaces of the Solar System. The low albedo asteroids of the outer region of the main belt and the Trojan group fall into the category

of so-called primitive objects because their surfaces are dark ($p_v \leq 0.05$) and redder than the sun. The surfaces of these bodies may be made of an irradiation mantle, originally rich in organic molecules. However, contrary to the similar primitive surface of at least one object that has recently moved into a Uranus-crossing orbits (5145 Pholus), their reflection spectra do not exhibit strong absorption bands in the 1.0- to 2.5-μm range. The surfaces of these objects have probably been altered by the solar flux and the organic molecules in their regoliths may have been dissociated. It is possible that the hydrocarbons have lost their hydrogen atoms and a carbon-rich crust covers the entire surface, although the red slopes of their reflection spectra remain to be explained.

None of the 18 surfaces observed in this study shows an absorption band in the 1.0- to 2.5-μm range similar to the ones present in the reflection spectrum of 5145 Pholus. Most of the objects observed have surfaces redder than the sun. Only 3200 Phaethon displays a blue-to-neutral reflectance spectrum in the near IR. Its surface apparently corresponds to a rubble-mantle from which volatiles have escaped due to the close proximity of the sun. Near-infrared spectroscopy extended to a wider number of ''primitive'' surfaces (small Trojan asteroids, Centaurs, cometary nuclei) will allow us to better understand the nature of the dark material from which they are made, as well as the processes that transform a red-primitive surface like Pholus into a blue-processed surface like 3200 Phaethon. There are other dormant-comet candidates, asteroids trapped into Earth-crossing orbits and/or associated with meteor showers for which we do not yet have near-infrared spectra, for example, 944 Hidalgo, 2101 Adonis, and 2212 Hephaistos. Also, a spectroscopic follow-up of cometary nuclei leaving the inner Solar System is needed in order to obtain a view of their inactive state and to derive the heliocentric variation of their reflectances.

ACKNOWLEDGMENTS

We thank D. C. Jewitt for his most valuable review of the manuscript and for providing the electronic version of the spectra of 5145 Pholus and 2060 Chiron published in Luu *et al.* (1994); D. J. Tholen for suggesting 72 Feronia as an interesting target for this study; B. Han and R. Whiteley for recording the spectrum of 3200 Phaethon; and K. Hoddap for providing the Argon lamp calibrations for the September 1995 data. We also thank the reviewers for their extremely valuable comments. This research was supported in part by NASA Grant NAGW 2650.

REFERENCES

Barucci, M. A., and M. Fulchignoni 1990. Pre- and Post-IRAS asteroid taxonomies. *Adv. Space Res.* **10**(3), 141–149.

Barucci, M. A., M. T. Capria, A. Coradini, and M. Fulchignoni 1987. Classification of asteroids using G-mode analysis. *Icarus* **72,** 304–324.

Barucci, M. A., M. Lazzarin, T. Owen, C. Barbieri, and M. Fulchignoni 1994. Near-infrared spectroscopy of dark asteroids. *Icarus* **110,** 287–291.

Bell, J. F., D. R. Davis, W. K. Hartmann, and M. J. Gaffey 1989. Asteroids: The big picture. In *Asteroids II* (R. P. Binzel, T. Gehrels, M. S. Matthews Eds.), pp. 921–948. Univ. of Arizona Press, Tucson.

Belton, M. J. S., H. Spinrad, P. A. Wehinger, and S. Wycroff 1985. *IAU Circ.* **4029.**

Britt, D. T., L. A. Lebofsky, and E. S. Howell 1992. The hydration state of main-belt C-class asteroids. *Bull. Am. Astron. Soc.* **3,** 940.

Cochran, A. L., and E. S. Baker 1984. Minor planet 1983 TB: A dead comet? *Icarus* **59,** 296–300.

Cruikshank, D. P. 1977. Radii and albedos of four trojan asteroids and jovian satellites VI and VII. *Icarus* **30,** 224–230.

Cruikshank, D. P. 1987. Dark matter in the Solar System. *Adv. Space Res.* **5**(7), 109–120.

Cruikshank, D. P., L. J. Allamandola, W. K. Hartmann, D. J. Tholen, R. H. Brown, C. N. Matthews, and J. F. Bell 1991. Solid C≡N bearing material on outer Solar System bodies. *Icarus* **94,** 345–353.

Cruikshank, D. P., L. V. Moroz, T. Geballe, C. M. Pieters, and J. F. Bell, III 1993. Asphaltite-like organics on Planetesimal 5145 Pholus. *Bull. Am. Astron. Soc.* **25,** 1125–1126.

Cruikshank, D. P., T. L. Roush, M. J. Bartholomew, L. V. Moroz, T. R. Geballe, S. M. White, J. F. Bell, III, Y. J. Pendleton, J. K. Davies, T. C. Owen, C. de Bergh, D. J. Tholen, M. P. Bernstein, R. H. Brown, and K. A. Tryka 1997. The composition of Planetesimal 5145 Pholus. *Icarus*, submitted.

Davies, J. K., J. Spencer, M. V. Sykes, and D. T. Tholen 1993a. *IAU Circ.* **5698.**

Davies, J. K., M. V. Sykes, and D. P. Cruikshank 1993b. Near-infrared photometry and spectroscopy of the unusual minor planet 5145 Pholus (1992 A.D.). *Icarus* **102,** 166–169.

Davies, J. K., D. J. Tholen, and D. R. Ballantyne 1996. Infrared observations of distant asteroids. *Astron. Soc. Pacific Proc.* **107,** 97–105.

Delsemme, A. H., and D. C. Miller 1971. Physico-chemical phenomena in comets. III. The continuum of Comet Burnham. *Planet. Space Sci.* **19,** 1229–1258.

Duncan, M., T. Quinn, and S. Tremaine 1988. The origin of short period comets. *Astrophys. J.* **328,** L69–L73.

Ferrari, C., and A. Brahic 1994. Azimuthal brightness asymmetries in planetary rings. I. Neptune's arc and narrow rings. *Icarus* **111,** 193–210.

Fink, U., M. Hoffman, W. Grundy, M. Hicks, and W. Sears 1992. The steep red spectrum of 1992 A.D.: An asteroid covered with organic material? *Icarus* **97,** 145–149.

Fitzsimmons, A., M. Dahlgren, C.-I. Lagerkvist, P. Magnusson, and I. P. Williams 1994. A spectroscopic survey of D-type asteroids. *Astron. Astrophys.* **282,** 634–642.

Gradie, J., and J. Veverka 1980. The composition of the trojan asteroids. *Nature* **283,** 840–842.

Gradie, J., and E. Tedesco 1982. Compositional structure of the asteroid belt. *Science* **216,** 1405–1407.

Halliday, I. 1988. Geminid fireballs and the peculiar asteroid 3200 Phaethon. *Icarus* **76,** 279–294.

Hahn, G., and M. Bailey 1990. Rapid dynamical evolution of giant Comet Chiron. *Nature* **348,** 132–136.

Hartmann, W. K., D. J. Tholen, and D. P. Cruikshank 1987. The relationship of active comets, ''extinct'' comets, and dark asteroids. *Icarus* **69,** 33–50.

Hartmann, W. K., D. J. Tholen, K. J. Meech, and D. P. Cruikshank 1990. 2060 Chiron—Colorimetry and cometary behavior. *Icarus* **83,** 1–15.

Hoddapp, K. W., J. L. Hora, E. Irwin, and T. Young 1994. KSPEC-A near infrared cross-dispersed spectrograph. *Pub. Astron. Soc. Pacific* **106,** 87–93.

Hoddapp, K. W., J. L. Hora, D. N. B. Hall, L. L. Cowie, M. Metzger, E. Irwin, K. Vural, L. J. Kozlowski, S. A. Cabelli, C. Y. Chen, D. E. Cooper, G. L. Bostrup, R. B. Bailey, and W. E. Kleinhans 1996. The HAWAII infrared detector arrays: Testing and astronomical characterization of prototype and science grade devices. *New Astron.* **1**(2), 177–196.

Hunt, J., K. Fox and I. P. Williams 1985. Asteroidal origin for the geminid meteor stream. In *Asteroids, Comets, Meteors II* (C.-I. Lagerkvist *et al.*, Eds.), pp. 549–553. Uppsala University.

Jewitt, D. C. and J. X. Luu 1990. CCD spectra of asteroids. II. The trojans as spectral analogs of cometary nuclei. *Astron. J.* **100**(3), 933–944.

Jones, T. D., L. A. Lebofsky, J. S. Lewis, and M. S. Marley 1990. The composition and origin of the C, P, and D asteroids: Water as a tracer of thermal evolution in the outer belt. *Icarus* **88,** 172–192.

Lazzarin, M., C. Barbieri, and M. A. Barucci 1995. Visible spectroscopy of dark, primitive asteroids. *Astron. J.* **110**(6), 3058–3072.

Lebofsky, L. A., T. D. Jones, P. D. Owensby, M. A. Feierberg, and G. J. Consolmagno 1990. The nature of the low-albedo asteroids from 3-μm multi-color photometry. *Icarus* **83,** 16–26.

Luu, J. 1991. CCD photometry and spectroscopy of the outer jovian satellites. *Astron. J.* **102**(3), 1213–1225.

Luu, J., and D. Jewitt 1996. Color diversity among the centaurs and Kuiper belt objects. *Astron. J.* **112**(5), 2310–2318.

Luu, J., D. Jewitt, and E. Cloutis 1994. Near-infrared spectroscopy of primitive Solar System objects. *Icarus* **109,** 133–144.

Meech, K. J. 1991. Outburst of Comet Halley at 14.3 AU. In *Reports of Planetary Astronomy,* p. 173. NASA Report N92-12792 03-89, Washington, DC.

Meech, K. J., and M. J. S. Belton 1990. The atmosphere of 2060 Chiron. *Astron. J.* **100**(4), 1323–1338.

Moroz, L. V., C. M. Pieters, and M. V. Akhmanova 1991. Spectroscopy of solid carbonaceous materials: Implications for dark surfaces of outer belt asteroids. *Proc. Lunar Planet. Sci. Conf.* **23,** 925–926.

Moroz, L. V., C. M. Pieters, and M. V. Akhmanova 1992. Why the surfaces of outer belt asteroids are dark and red? *Proc. Lunar Planet. Sci.* **23,** 931–932.

Mueller, B. E. A. 1992. *IAU Circ.* **5434.**

Notesco, G. and A. Bar-Nun 1996. Enrichment of CO over N_2 by their trapping in amorphous ice and implications to Comet P/Halley. *Icarus* **122,** 118–121.

Owen, T., D. P. Cruikshank, C. de Bergh, and T. Geballe 1995. Dark matter in the outer Solar System. *Adv. Space Res.* **16**(2), 41–49.

Porco, C. C., P. D. Nicholson, J. N. Cuzzi, J. J. Lissauer, and L. W. Esposito 1995. Neptune's ring system. In *Neptune and Triton* (D. P. Cruikshank, Ed.), pp. 703–804. Univ. of Arizona Press, Tucson.

Ramsay, S. K., C. M. Mountain, and T. R. Geballe 1992. Non-thermal emission in the atmosphere above Mauna Kea. *Mon. Not. R. Astron. Soc.* **259,** 751–760.

Tedesco, E. F., G. J. Veeder, J. W. Fowler, and J. R. Chillemi 1992. The IRAS Minor Planet Survey. JPL Report PL-TR-92-2049.

Tholen, D. J. 1992. *IAU Circ.* **5434.**

Tholen, D. J., and B. Zellner 1984. Multicolor photometry of outer jovian satellites. *Icarus* **58,** 246–253.

Tholen, D. J., and M. A. Barucci 1989. Asteroid taxonomy. In *Asteroids II* (R. P. Binzel, T. Gehrels, and M. S. Matthews, Eds.), pp. 298–315. Univ. of Arizona Press, Tucson.

Thomas, P. C., J. Veverka, and P. Helfenstein 1995. Neptune's small satellites. In *Neptune and Triton* (D. P. Cruikshank, Ed.), pp. 685–699. Univ. of Arizona Press, Tucson.

Thompson, W. R., B. G. Murray, B. N. Khare, and C. Sagan 1987. Coloration and darkening of methane clathrate and other ices by charged particle irradiation: Applications to the outer Solar System. *J. Geophys. Res.* **92,** 14,933–14,947.

Veeder, G. J., C. Kowal, and D. L. Matson 1984. The earth-crossing asteroid 1983 TB. *Lunar Planet. Sci.* **15,** 878–879.

Vilas, F. and B. A. Smith 1985. Reflectance spectrophotometry (~0.5–1.0 μm) of outer-belt asteroids: Implications for primitive, organic Solar System material. *Icarus* **64,** 503–516.

Williams, I. P., and Z. Wu 1993. The geminid meteor stream and asteroid 3200 Phaethon. *Mon. Not. R. Astron. Soc.* **262,** 231–248.

Whipple, F. L. 1950. A comet model. I. The acceleration of Comet Encke. *Astrophys. J.* **111,** 375–394.

Whipple, F. L. 1983. *IAU Circ.* **3881.**

Wilson, P. D., C. Sagan, and W. R. Thompson 1994. The organic surface of 5145 Pholus: Constraints set by scattering theory. *Icarus* **107,** 288–303.

Zellner, B., D. J. Tholen, and E. F. Tedesco 1985. The eight-color asteroid survey: Results for 589 minor planets. *Icarus* **61,** 355–416.